PDE-Driven Adaptive Morphology for Matrix Fields

Bernhard Burgeth, Michael Breuß, Luis Pizarro, and Joachim Weickert

Mathematical Image Analysis Group, Faculty of Mathematics and Computer Science, Saarland University, 66041 Saarbrücken, Germany
{burgeth,breuss,pizarro,weickert}@mia.uni-saarland.de
http://www.mia.uni-saarland.de

Abstract. Matrix fields are important in many applications since they are the adequate means to describe anisotropic behaviour in image processing models and physical measurements. A prominent example is diffusion tensor magnetic resonance imaging (DT-MRI) which is a medical imaging technique useful for analysing the fibre structure in the brain. Recently, morphological partial differential equations (PDEs) for dilation and erosion known for grey scale images have been extended to three dimensional fields of symmetric positive definite matrices.

In this article we propose a novel method to incorporate adaptivity into the matrix-valued, PDE-driven dilation process. The approach uses a structure tensor concept for matrix data to steer anisotropic morphological evolution in a way that enhances and completes line-like structures in matrix fields. Numerical experiments performed on synthetic and real-world data confirm the gap-closing and line-completing qualities of the proposed method.

1 Introduction

Initiated in the sixties by the pioneering research of Serra and Matheron on binary morphology [23, 31], this branch of image processing has developed into a rich field of research. Numerous monographs e.g. [17, 24, 32, 33, 34] and proceedings, e.g. [16,18,22] bear witness to the variety in mathematical morphology. The building blocks of morphological operations are dilation and erosion. These are usually realised by algebraic set operations involving a probing set, a so-called structuring element, e.g. [34] for details. An alternative approach to dilation is given [1] by the nonlinear partial differential equation (PDE)

$$\partial_t u = \|\nabla u\| = \sqrt{|\partial_x u|^2 + |\partial_y u|^2} \tag{1}$$

with initial condition $u(x, y, 0) = f(x, y)$. The equation mimics the dilation of a grey scale image f with respect to a ball-shaped structuring element of growing radius t. PDEs of this type using a continuous size parameter t for the structuring element give rise to *continuous-scale morphology* [1,2,6,29,35]. Equation (1) has been extended in two ways:

X.-C. Tai et al. (Eds.): SSVM 2009, LNCS 5567, pp. 247–258, 2009.

Firstly, in [5] *adaptivity* has been incorporated by introducing a speed function $\beta = \beta(u)$ into (1),

$$\partial_t u = \beta(u) \cdot \|\nabla u\| \tag{2}$$

Earlier attempts towards adaptivity have been made in [20, 26] where a local switch between dilation and erosion with a nonadaptive structuring element leads to a so-called morphological shock filter, and in [21] introducing morphological amoebae described in a set-theoretic framework.

Secondly, in [8] scalar continuous morphology has been extended to a PDE-driven morphology of matrix-valued images, *matrix fields* for short.

Matrix fields have received increasing attention over the recent years since they are the appropriate data type to describe anisotropy in models or measurements of physical quantities. For instance, diffusion tensor magnetic resonance imaging (DT-MRI) became a valuable tool in medicine for in vivo diagnosis. It results in three dimensional tensor fields that describe the diffusive properties of water molecules, and as such the structure of the tissue under examination.

The goal of this article is to introduce adaptivity into morphology for matrix fields. As it turns out it is advantageous to start for this generalisation from a scalar adaptive formulation for d-dimensional data u in form of the PDE

$$\partial_t u = \|M(u) \cdot \nabla u\| \tag{3}$$

with ∇u as a column vector and a data dependent, symmetric, positive semidefinite $d \times d$-matrix $M = M(u)$ rather than from (2). For example, for greyvalue images ($d = 2$) one has $M = \begin{pmatrix} a & b \\ b & c \end{pmatrix}$ and (3) turns into

$$\partial_t u = \sqrt{(a\partial_x u + b\partial_y u)^2 + (b\partial_x u + c\partial_y u)^2} \tag{4}$$

An application of the mapping $(x, y)^\top \mapsto M(x, y)^\top$ transforms a sphere centered around the origin into an ellipse. So, in fact, (3) describes a dilation with an ellipsoidal structuring element. The matrix M must contain directional information of the evolving u, and thus it may be derived from the so-called structure tensor. The structure tensor, going back to [14, 27, 4], is a classic tool in image processing to extract directional information from an image. It is given by

$$S_\rho(u(x)) := G_\rho * \left(\nabla u(x) \cdot (\nabla u(x))^\top\right) = \left(G_\rho * \left(\partial_{x_i} u(x) \cdot \partial_{x_j} u(x)\right)\right)_{i,j=1,\ldots,d} \tag{5}$$

Here $G_\rho *$ indicates a convolution with a Gaussian of standard deviation ρ, however, more general averaging procedures can be used. For more details the reader is referred to [3] and the literature cited there.

We will make use of the extended structure tensor concept for matrix fields as proposed in [10]. There it was used to steer an coherence-enhancing diffusion process for matrix fields, an anisotropic filtering process that has been proposed for scalar and colour images in [36, 37].

In [38, 7, 13] Di Zenzo's approach [12] to construct a structure tensor for multi-channel images has been extended to matrix fields yielding a standard structure tensor (using the notation of forthcoming Section 2): $J_\rho(U(x)) := \sum_{i,j=1}^{m} S_\rho(U_{i,j}(x))$ This construction has been refined to a customisable structure tensor in [30].

The article has the following structure: We will briefly convey in Section 2 basic notions of matrix analysis needed to establish a matrix-valued PDE for an adaptively steered morphological dilation process. This includes a short account of the construction of an extended structure tensor for matrix fields. In Section 3 we introduce the steering tensor that guides the dilation process adaptively. We explain how the numerical scheme of Rouy and Tourin is generalised to the matrix valued setting in Section 4. We compare in our experiments adaptive and isotropic dilation with CED-diffusion when applied to synthetic matrix fields and real DT-MRI data sets. We report on this comparison of the results in Section 5. The remarks in Section 6 conclude this article.

2 Matrix Analysis and an Extended Structure Tensor Concept

This section contains the key definitions for the formulation of matrix-valued PDEs. For a more detailed exposition the reader is referred to [9].

A matrix field is considered as a mapping $U : \Omega \subset \mathbb{R}^d \longrightarrow \mathrm{Sym}_m(\mathbb{R})$ from a d-dimensional image domain into the set of symmetric $m \times m$-matrices with real entries, $U(x) = (U_{p,q}(x))_{p,q=1,\ldots,m}$. The set of positive (semi-) definite matrices, denoted by $\mathrm{Sym}_m^{++}(\mathbb{R})$ (resp., $\mathrm{Sym}_m^{+}(\mathbb{R})$), consists of all symmetric matrices A with $\langle v, Av\rangle := v^\top Av > 0 \quad (\text{resp.}, \geq 0) \quad \text{for} \quad v \in \mathbb{R}^m \setminus \{0\}$. This set is of special interest since DT-MRI produces data with this property. Note that at each point x the matrix $U(x)$ of a field of symmetric matrices can be diagonalised yielding $U(x) = V(x)^\top D(x)V(x)$, where $V(x)$ is a orthogonal matrix, while $D(x)$ is a diagonal matrix. In the sequel we will denote $m \times m$ - diagonal matrices with entries $\lambda_1, \ldots, \lambda_m \in \mathbb{R}$ from left to right simply by $\mathrm{diag}(\lambda_i)$.

The extension of a function $h : \mathbb{R} \longrightarrow \mathbb{R}$ to $\mathrm{Sym}_m(\mathbb{R})$ is standard [19]: With a slight abuse of notation we set $h(U) := V^\top \mathrm{diag}(h(\lambda_1), \ldots, h(\lambda_m))V \in \mathrm{Sym}_m^{+}(\mathbb{R})$, h denoting now a function acting on matrices as well. Specifying $h(s) = |s|, s \in \mathbb{R}$ as the absolut value function leads to the absolut value $|A| \in \mathrm{Sym}_m^{+}(\mathbb{R})$ of a matrix A. It is natural to define the partial derivative for matrix fields *componentwise*:

$$\overline{\partial}_\omega U = (\partial_\omega U_{p,q})_{p,q=1,\ldots,m} \tag{6}$$

where $\omega \in \{t, x_1, \ldots, x_d\}$, that is, $\overline{\partial}_\omega$ stands for a spatial or temporal derivative. Viewing a matrix as a tensor (of second order), its gradient would be a third order tensor according to the rules of differential geometry. However, we adopt a more operator-algebraic point of view by defining the *generalised gradient* $\overline{\nabla} U(x)$ at a voxel $x = (x_1, \ldots, x_d)$ by

$$\overline{\nabla} U(x) := (\overline{\partial}_{x_1} U(x), \ldots, \overline{\partial}_{x_d} U(x))^\top \tag{7}$$

which is an element of $(\mathrm{Sym}_m(\mathbb{R}))^d$, in close analogy to the scalar setting where $\nabla u(x) \in \mathbb{R}^d$. For $W \in (\mathrm{Sym}_m(\mathbb{R}))^d$ we set $|W|_p := \sqrt[p]{|W_1|^p + \cdots + |W_d|^p}$ for $0 < p < +\infty$. It results in a positive semidefinite matrix from $\mathrm{Sym}_m^+(\mathbb{R})$, the direct counterpart of a nonnegative real number as the length of a vector in $\mathbb{R}^d$.

There will be the need for a symmetric multiplication of symmetric matrices. We opt for the so-called Jordan product $A \bullet_J B := \frac{1}{2}(AB + BA)$. It produces a symmetric matrix, and it is commutative but neither associative nor distributive.

Furthermore, for later use in numerical schemes we have to clarify the notion of maximum and minimum of two symmetric matrices A, B. In direct anaology with relations known to be valid for real numbers one defines [8]:

$$\max(A,B) = \frac{1}{2}(A + B + |A - B|) \text{ and } \min(A,B) = \frac{1}{2}(A + B - |A - B|) \quad (8)$$

where $|F|$ stands for the absolut value of the matrix F.

With this at our disposal we formulate the matrix-valued counterpart of (3) as

$$\overline{\partial}_t U = |\overline{M}(U) \bullet \overline{\nabla} U|_2 \quad (9)$$

with an initial matrix field $F(x) = U(x,0)$. Here $\overline{M}(U)$ denotes a symmetric $md \times md$-block matrix with d^2 blocks of size $m \times m$ that is multiplied block-wise with $\overline{\nabla} U$ employing the symmetrised product "$\bullet$". Note that $|\cdot|_2$ stands for the length of $\overline{M}(U) \bullet \overline{\nabla} U$ in the matrix valued sense. The construction of $\overline{M}(U)$ is detailed in Section 3 and relies on the so-called *full structure tensor*.

The full structure tensor $\overline{\mathcal{S}}_L$ for matrix fields as defined in [10] reads

$$\overline{\mathcal{S}}_L(U) := G_\rho * \left(\overline{\nabla} U \cdot (\overline{\nabla} U)^\top\right) = \left(G_\rho * \left(\overline{\partial}_{x_i} U \cdot \overline{\partial}_{x_j} U\right)\right)_{i,j=1,\ldots,d} \quad (10)$$

with $G_\rho *$ indicating a convolution with a Gaussian of standard deviation ρ.

$\overline{\mathcal{S}}_L(U(x))$ is a symmetric $md \times md$-block matrix with d^2 blocks of size $m \times m$, $\overline{\mathcal{S}}_L(U(x)) \in \mathrm{Sym}_d(\mathrm{Sym}_m(\mathbb{R})) = \mathrm{Sym}_{md}(\mathbb{R})$. Typically for the 3D medical DT-MRI data one has $d = 3$ and $m = 3$, yielding a 9×9-matrix $\overline{\mathcal{S}}_L$. It can be diagonalised as $\overline{\mathcal{S}}_L(U) = \sum_{k=1}^{md} \lambda_k w_k w_k^\top$ with real eigenvalues λ_k (w.l.o.g. arranged in decreasing order) and an orthonormal basis $\{w_k\}_{k=1,\ldots,md}$ of $\mathbb{R}^{md}$.

In order to extract useful d-dimensional directional information $\overline{\mathcal{S}}_L(U) \in \mathrm{Sym}_{md}(\mathbb{R})$ is reduced to a structure tensor $S(U) \in \mathrm{Sym}_d(\mathbb{R})$ in a generalised projection step [10] using the block operator matrix $\mathrm{Tr}_A := \mathrm{diag}(\mathrm{tr}_A, \ldots, \mathrm{tr}_A)$ containing the trace operation. We set $\mathrm{Tr} := \mathrm{Tr}_{I_m}$ where I_m denotes the $m \times m$ unit matrix. This operator matrix acts on elements of the space $(\mathrm{Sym}_m(\mathbb{R}))^d$ as well as on block matrices via formal block-wise matrix multiplication,

$$\begin{pmatrix} \mathrm{tr}_A & \cdots & 0 \\ \vdots & \ddots & \vdots \\ 0 & \cdots & \mathrm{tr}_A \end{pmatrix} \begin{pmatrix} M_{11} & \cdots & M_{1d} \\ \vdots & \ddots & \vdots \\ M_{d1} & \cdots & M_{dd} \end{pmatrix} = \begin{pmatrix} \mathrm{tr}_A(M_{11}) & \cdots & \mathrm{tr}_A(M_{1d}) \\ \vdots & \ddots & \vdots \\ \mathrm{tr}_A(M_{d1}) & \cdots & \mathrm{tr}_A(M_{dd}) \end{pmatrix}, \quad (11)$$

provided that the square blocks M_{ij} have the same size as A. The projection that is conveyed by the reduction process condenses the directional information contained in $\overline{\mathcal{S}}_L(U)$, for a more detailed reasoning we must refer the reader to [10]

for the sake of brevity. The reduction operation is accompanied by an extension operation: The I_m-extension is the mapping from $\mathrm{Sym}_d(\mathbb{R})$ to $\mathrm{Sym}_{md}(\mathbb{R})$ conveyed by the *Kronecker product* $\otimes$:

$$\begin{pmatrix} v_{11} & \cdots & v_{1d} \\ \vdots & \ddots & \vdots \\ v_{d1} & \cdot & v_{dd} \end{pmatrix} \longmapsto \begin{pmatrix} v_{11} & \cdots & v_{1d} \\ \vdots & \ddots & \vdots \\ v_{d1} & \cdots & v_{dd} \end{pmatrix} \otimes \begin{pmatrix} I_m & \cdots & I_m \\ \vdots & \ddots & \vdots \\ I_m & \cdots & I_m \end{pmatrix} := \begin{pmatrix} v_{11}I_m & \cdots & v_{1d}I_m \\ \vdots & \ddots & \vdots \\ v_{d1}I_m & \cdots & v_{dd}I_m \end{pmatrix} \quad (12)$$

This resizing step renders a proper matrix-vector multiplication with the large generalised gradient $(\overline{\nabla}U(x))^\top$ possible. By specifying the matrix A in (11) one may invoke a priori knowledge into the direction estimation [10]. The research on these structure-tensor concepts has been initiated by [38, 7]. The approaches to matrix field regularisation suggested in [11] are based on differential geometric considerations. Comprehensive survey articles on the analysis of matrix fields using various techniques can be found in [39].

3 Steering Matrix $\overline{M}(U)$ for Matrix Fields

With this notions we are in the position to propose the steering matrix $\overline{M}$ in the adaptive dilation process for matrix fields. We proceed in four steps:

1. The matrix field $\mathbb{R}^d \ni x \mapsto U(x)$ provides us with a module field of generalised gradients $\overline{\nabla}U(x)$ from which we construct the generalised structure tensor $\overline{\mathcal{S}}_L\,(U(x))$ possibly with a certain integration scale ρ. This step corresponds exactly to the scalar case.
2. We infer d-dimensional directional information by reducing $\overline{\mathcal{S}}_L\,(U(x))$ with tr_A by means of the block operator matrix Tr_A leading to a symmetric $d \times d$-matrix S, for example $S = J_\rho$ if $A = I_m$,
$$S(x) := \mathrm{Tr}_A\big(\overline{\mathcal{S}}_L\,(U(x))\big) \quad (13)$$
3. The symmetric $d \times d$-matrix S is spectrally decomposed, and the following mapping is applied:
$$H : \begin{cases} \mathbb{R}^d_+ \longrightarrow \mathbb{R}^d \\ (\lambda_1, \ldots, \lambda_d) \longmapsto \frac{c}{\lambda_1 + \cdots + \lambda_d}(\lambda_d, \lambda_{d-1}, \ldots, \frac{K}{c} \cdot \lambda_1) \end{cases}, \quad (14)$$
with constants $c, K > 0$. H applied to S yields the steering matrix M,
$$M := H(S) \quad (15)$$
Observe that the ellipsoid associated with the matrix M is flipped if compared with S and, depending on the choice of K, more excentric than the one accompanying S.
4. Finally we enlarge the $d \times d$-matrix M to a $md \times md$-matrix $\overline{M}$ by the extension operation:
$$\overline{M} = M \otimes \begin{pmatrix} I_m & \cdots & I_m \\ \vdots & \ddots & \vdots \\ I_m & \cdots & I_m \end{pmatrix} \quad (16)$$

4 Matrix-Valued Numerical Schemes

In the context of PDE-based mathematical morphology, first-order finite difference methods such as the *Osher-Sethian scheme* [25] and the *Rouy-Tourin method* [28] are reasonable choices for solving the scalar PDE (4). We choose the latter in our experiments. The variant we present for the sake of brevity in its two-dimensional form reads

$$u_{i,j}^{n+1} = u_{i,j}^{n} + \tau \left(\max\left(\frac{1}{h_x} \max\left(-D_-^x u_{i,j}^n, 0\right) , \frac{1}{h_x} \max\left(D_+^x u_{i,j}^n, 0\right) \right)^2 \right.$$
$$\left. + \quad \max\left(\frac{1}{h_y} \max\left(-D_-^y u_{i,j}^n, 0\right) , \frac{1}{h_y} \max\left(D_+^y u_{i,j}^n, 0\right) \right)^2 \right)^{1/2} \quad (17)$$

In the latter formulation we employ the notation u_{ij}^n as the grey value of the image u at the pixel centred at $(ih_x, jh_y) \in \mathbb{R}^2$ at the time-level $n\tau$ of the

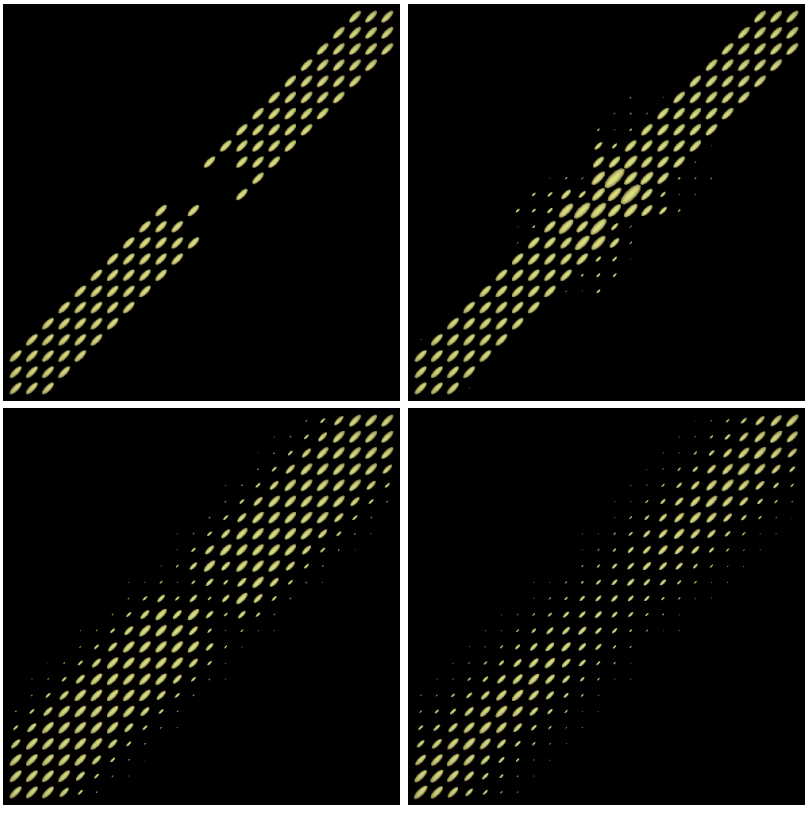

Fig. 1. (a) Top left: 2D slice of original 3D matrix field. **(b) Top right:** Adaptive dilation with of the original data with $K = 25, \rho = 1$ after $t = 0.3$. **(c) Bottom left:** Standard PDE-based dilation mimicing a ball-shaped structuring element after $t = 1$. **(d) Bottom right:** CED-filtering with $\rho = 4$ after $t = 10$.

evolution. Additionally we use standard abbreviations for forward and backward difference operators, i.e., $D_+^x u_{i,j}^n := u_{i+1,j}^n - u_{i,j}^n$ and $D_-^x u_{i,j}^n := u_{i,j}^n - u_{i-1,j}^n$. and spatial grid size h_x, h_y. This scheme approximates, in the pixel (ih_x, jh_y)

$$u_x \approx \max\left(\frac{1}{h_x}\max\left(-D_-^x u_{i,j}^n, 0\right), \frac{1}{h_x}\max\left(D_+^x u_{i,j}^n, 0\right)\right) \tag{18}$$

$$u_y \approx \max\left(\frac{1}{h_y}\max\left(-D_-^y u_{i,j}^n, 0\right), \frac{1}{h_y}\max\left(D_+^y u_{i,j}^n, 0\right)\right) \tag{19}$$

Using this approximations, we modify the original Rouy-Tourin scheme (17) in an obvious manner to obtain a numerical scheme for the adaptive version of the PDE-based dilation (3). The extension to higher dimensions poses no problem. Since linear combinations and elementary functions such as the square, square-root or absolute value function for matrix fields are now at our disposal it is straightforward to define one sided differences in x-direction for 2D matrix fields of $m \times m$-matrices:

$$D_+^x U^n(i,j) := U^n((i+1)h_x, jh_y) - U^n(ih_x, jh_y) \in \mathrm{Sym}_m(\mathbb{R}) \tag{20}$$

$$D_-^x U^n(i,j) := U^n(ih_x, jh_y) - U^n((i-1)h_x, jh_y) \in \mathrm{Sym}_m(\mathbb{R}) \tag{21}$$

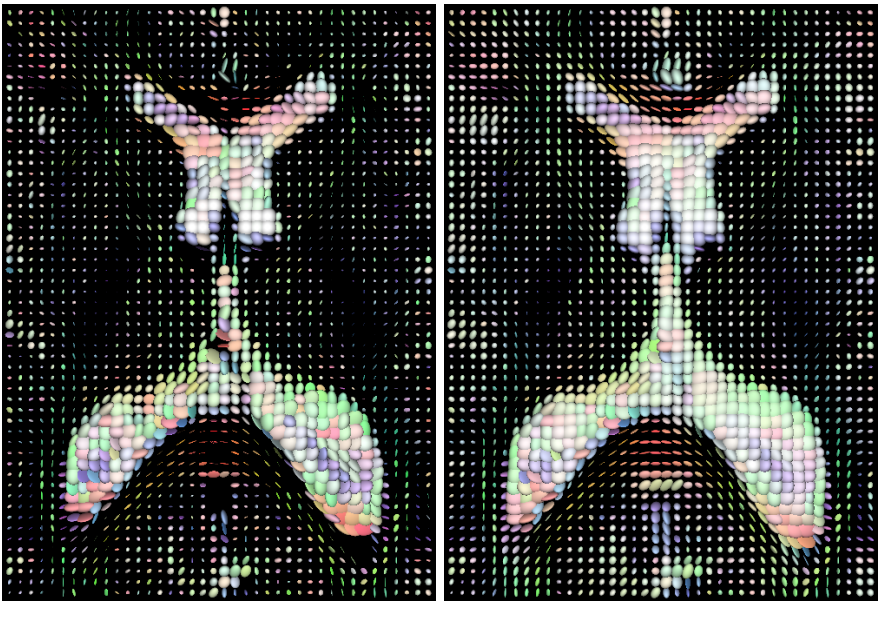

Fig. 2. (a) Left: 2D slice of 3D DT-MRI data set. **(b) Right:** Adaptive dilation of the original data with $K = 10$, $\rho = 1$, $t = 0.5$.

In order to avoid confusion with the subscript notation for matrix components we used the notation $U(i,j)$ to indicate the (matrix-) value of the matrix field evaluated at the voxel centred at $(ih_x, jh_y) \in \mathbb{R}^2$. The y-direction (and z-direction in 3D) is treated accordingly. The notion of supremum and infimum of two matrices – as needed in a matrix variant of Rouy-Tourin – has been provided by (8). Having these generalisations at our disposal a modified, adaptive version of the Rouy-Tourin scheme is available now in the setting of matrix fields simply by replacing grey values u_{ij}^n by matrices $U^n(i,j)$.

5 Experiments

The matrix data are visualised as an ellipsoid in each voxel via the level sets of quadratic form $\{v \in \mathbb{R}^2 v : v^\top U^{-2}(i,j)v = const.\}$ associated with the matrix

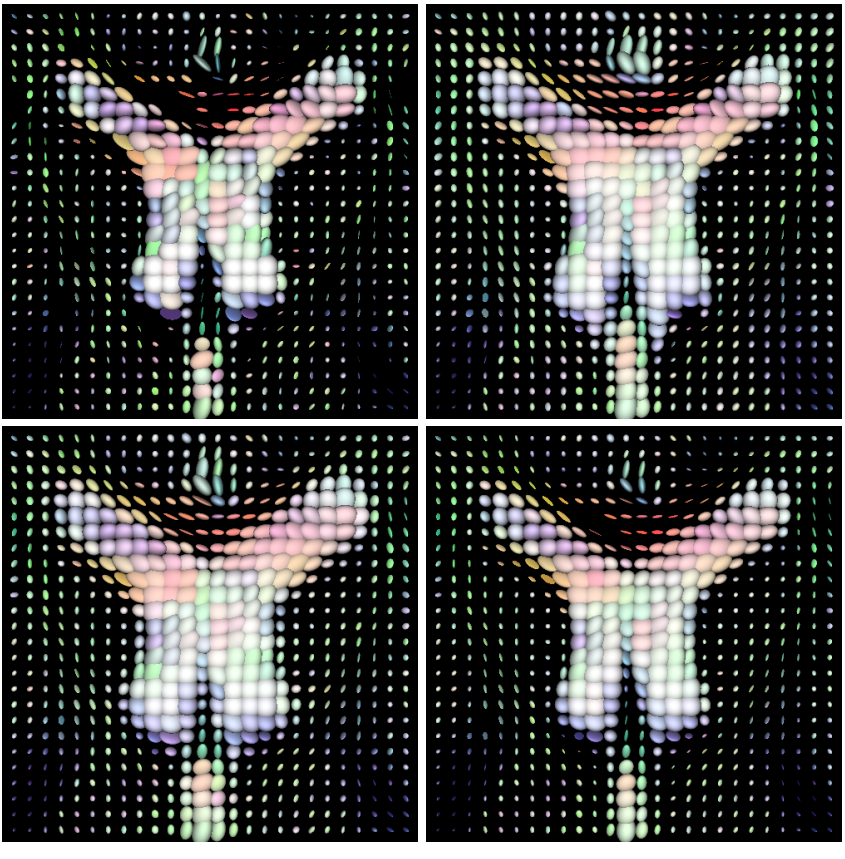

Fig. 3. (a) Top left: Enlarged section of the original data of figure 2 showing the *genu* area. **(b) Top right:** Adaptive dilation of the original data with $K = 10$, $\rho = 1$, $t = 0.5$. **(c) Bottom left:** Standard PDE-based dilation mimicing a ball-shaped structuring element with $t = 0.5$. **(d) Bottom right:** CED-filtering with $\rho = 1$ after $t = 0.5$.

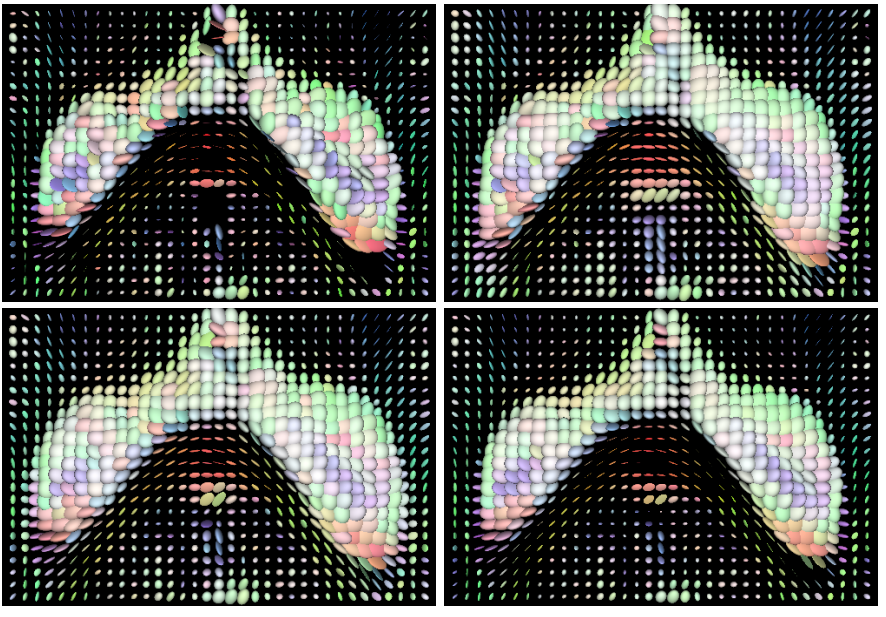

Fig. 4. (a) Top left: Enlarged section of the original data of figure 2 showing the *splenium* area. **(b) Top right:** Adaptive dilation of the original data with $K = 10$, $\rho = 1$, $t = 0.5$. **(c) Bottom left:** Standard PDE-based dilation mimicing a ball-shaped structuring element with $t = 0.5$. **(d) Bottom right:** CED-filtering with $\rho = 1$ after $t = 0.5$.

$U(i,j) \in \mathrm{Sym}_3^+(\mathbb{R})$ representing the matrix field at voxel (ih_x, jh_y). By using U^{-2} the length of the semi-axes of the ellipsoid correspond directly with the three eigenvalues of the matrix. Changing the constant *const.* amounts to a mere scaling of the ellipsoids. Note that only positive definite matrices produce ellipsoids as level sets of its quadratic form. In all our experiments we compare the results of the proposed matrix-valued adaptive dilation with the isotropic dilation [8] , and with the matrix-valued coherence-enhancing diffusion from [10]. For the explicit numerical schemes we used a time step size of 0.1, grid size $h_x = h_y = 1$, and $c = 0.01 \cdot K$ in (14).

Figure 1 shows a synthetic data set of size 32×32 representing an interrupted diagonal stripe built from cigar-shaped ellipsoids of equal size.

All methods succeed to some degree to fill the gaps. In the case of the proposed adaptive dilation the gap is filled almost completely with tensors comparable in size with the original ones while the width of the stripe is not altered at all. However, the numerical scheme has a slight bias towards the directions of the coordinate system entailing in the appearance of mild artefacts. Standard dilation fills the gap basically as a side effect of the isotropic dilation process which leads also to a considerable widening of the ribbon-like structure. CED for matrix fields produces indeed small cigar-shaped ellipsoids at the location of the gap. But the process is considerably slower than any of the dilation processes

and the neighbouring ellipsoids become smaller due to the property of mass conservation. Additionally an undesirable widening of the stripe is observed.

We also tested the proposed method on a real DT-MRI data set of a human head consisting of a $128 \times 128 \times 38$-field of positive definite matrices. Figure 2 shows the lateral ventricals in a 40×55 2D section before and after applying adaptive dilation with speed parameter $K = 10$, integration scale $\rho = 1$ and stopping time $t = 0.5$. For a better comparison we display two enlarged regions of interest in Figures 3 and 4, namely the *genu* and the *splenium* areas, resp.. We observe that adaptive dilation preserves the shape of the ventricles better than the isotropic dilation, while enhancing slightly the directional structure of the fibre tracts surrounding the ventricles. Due to measurement errors the fibre tracts are interrupted in the original Figures 3(a) and 4(a). These holes in the anisotropic regions (splenium) are quickly filled by the adaptive dilation while CED-filtering will take much longer to do so.

6 Conclusion

In this article we have presented a novel method for an adaptive, PDE-based dilation process in the setting of matrix fields. The evolution governed by a matrix-valued PDE is guided by a steering tensor, the construction of which relies on an extended structure tensor concept for matrix fields. A matrix-valued extension of the Rouy-Tourin-scheme that allows to include directional information is employed to solve the novel PDE. Experiments on positive semidefinite DT-MRI and synthetic data confirm that the novel adaptive dilation process displays line-enhancing and gap-closing qualities, and as such it is superior to standard isotropic dilation which extends structures in all directions. It is also a valuable alternative in terms of quality and speed to coherence-enhancing diffusion filtering for matrix fields, an anisotropic processes which aims at enhancing flow-like structures as well but may suffer from dissipative effects. Future research will concentrate on improving the numerical realisation of our adaptive dilation.

Acknowledgement

The financial support of the German Academic Exchange Service (DAAD) for the third author is gratefully acknowledged.

References

1. Alvarez, L., Guichard, F., Lions, P.-L., Morel, J.-M.: Axioms and fundamental equations in image processing. Archive for Rational Mechanics and Analysis 123, 199–257 (1993)
2. Arehart, A.B., Vincent, L., Kimia, B.B.: Mathematical morphology: The Hamilton–Jacobi connection. In: Proc. Fourth International Conference on Computer Vision, Berlin, pp. 215–219. IEEE Computer Society Press, Los Alamitos (1993)

3. Bigün, J.: Vision with Direction. Springer, Berlin (2006)
4. Bigün, J., Granlund, G.H., Wiklund, J.: Multidimensional orientation estimation with applications to texture analysis and optical flow. IEEE Transactions on Pattern Analysis and Machine Intelligence 13(8), 775–790 (1991)
5. Breuß, M., Burgeth, B., Weickert, J.: Anisotropic continuous-scale morphology. In: Martí, J., Benedí, J.M., Mendonça, A.M., Serrat, J. (eds.) IbPRIA 2007. LNCS, vol. 4478, pp. 515–522. Springer, Heidelberg (2007)
6. Brockett, R.W., Maragos, P.: Evolution equations for continuous-scale morphological filtering. IEEE Transactions on Signal Processing 42, 3377–3386 (1994)
7. Brox, T., Weickert, J., Burgeth, B., Mrázek, P.: Nonlinear structure tensors. Image and Vision Computing 24(1), 41–55 (2006)
8. Burgeth, B., Bruhn, A., Didas, S., Weickert, J., Welk, M.: Morphology for tensor data: Ordering versus PDE-based approach. Image and Vision Computing 25(4), 496–511 (2007)
9. Burgeth, B., Didas, S., Florack, L., Weickert, J.: A generic approach to diffusion filtering of matrix-fields. Computing 81, 179–197 (2007)
10. Burgeth, B., Didas, S., Weickert, J.: A general structure tensor concept and coherence-enhancing diffusion filtering for matrix fields. Technical Report 197, Department of Mathematics, Saarland University, Saarbrücken, Germany (July 2007); to appear in: Laidlaw, D., Weickert, J. (eds.): Visualization and Processing of Tensor Fields. Springer, Heidelberg (2009)
11. Chefd'Hotel, C., Tschumperlé, D., Deriche, R., Faugeras, O.: Constrained flows of matrix-valued functions: Application to diffusion tensor regularization. In: Heyden, A., Sparr, G., Nielsen, M., Johansen, P. (eds.) ECCV 2002. LNCS, vol. 2350, pp. 251–265. Springer, Heidelberg (2002)
12. Di Zenzo, S.: A note on the gradient of a multi-image. Computer Vision, Graphics and Image Processing 33, 116–125 (1986)
13. Feddern, C., Weickert, J., Burgeth, B., Welk, M.: Curvature-driven PDE methods for matrix-valued images. International Journal of Computer Vision 69(1), 91–103 (2006)
14. Förstner, W., Gülch, E.: A fast operator for detection and precise location of distinct points, corners and centres of circular features. In: Proc. ISPRS Intercommission Conference on Fast Processing of Photogrammetric Data, Interlaken, Switzerland, June 1987, pp. 281–305 (1987)
15. Goutsias, J., Heijmans, H.J.A.M., Sivakumar, K.: Morphological operators for image sequences. Computer Vision and Image Understanding 62, 326–346 (1995)
16. Goutsias, J., Vincent, L., Bloomberg, D.S. (eds.): Mathematical Morphology and its Applications to Image and Signal Processing. Computational Imaging and Vision, vol. 18. Kluwer, Dordrecht (2000)
17. Heijmans, H.J.A.M.: Morphological Image Operators. Academic Press, Boston (1994)
18. Heijmans, H.J.A.M., Roerdink, J.B.T.M. (eds.): Mathematical Morphology and its Applications to Image and Signal Processing. Computational Imaging and Vision, vol. 12. Kluwer, Dordrecht (1998)
19. Horn, R.A., Johnson, C.R.: Matrix Analysis. Cambridge University Press, Cambridge (1990)
20. Kramer, H.P., Bruckner, J.B.: Iterations of a non-linear transformation for enhancement of digital images. Pattern Recognition 7, 53–58 (1975)
21. Lerallut, R., Decencière, E., Meyer, F.: Image filtering using morphological amoebas. Image and Vision Computing 25(4), 395–404 (2007)

22. Louverdis, G., Vardavoulia, M.I., Andreadis, I., Tsalides, P.: A new approach to morphological color image processing. Pattern Recognition 35, 1733–1741 (2002)
23. Matheron, G.: Eléments pour une théorie des milieux poreux. Masson, Paris (1967)
24. Matheron, G.: Random Sets and Integral Geometry. Wiley, New York (1975)
25. Osher, S., Fedkiw, R.P.: Level Set Methods and Dynamic Implicit Surfaces. Applied Mathematical Sciences, vol. 153. Springer, New York (2002)
26. Osher, S., Sethian, J.A.: Fronts propagating with curvature-dependent speed: Algorithms based on Hamilton–Jacobi formulations. Journal of Computational Physics 79, 12–49 (1988)
27. Rao, A.R., Schunck, B.G.: Computing oriented texture fields. CVGIP: Graphical Models and Image Processing 53, 157–185 (1991)
28. Rouy, E., Tourin, A.: A viscosity solutions approach to shape-from-shading. SIAM Journal on Numerical Analysis 29, 867–884 (1992)
29. Sapiro, G., Kimmel, R., Shaked, D., Kimia, B.B., Bruckstein, A.M.: Implementing continuous-scale morphology via curve evolution. Pattern Recognition 26, 1363–1372 (1993)
30. Schultz, T., Burgeth, B., Weickert, J.: Flexible segmentation and smoothing of DT-MRI fields through a customizable structure tensor. In: Bebis, G., Boyle, R., Parvin, B., Koracin, D., Remagnino, P., Nefian, A., Meenakshisundaram, G., Pascucci, V., Zara, J., Molineros, J., Theisel, H., Malzbender, T. (eds.) ISVC 2006. LNCS, vol. 4291, pp. 455–464. Springer, Heidelberg (2006)
31. Serra, J.: Echantillonnage et estimation des phénomènes de transition minier. PhD thesis, University of Nancy, France (1967)
32. Serra, J.: Image Analysis and Mathematical Morphology, vol. 1. Academic Press, London (1982)
33. Serra, J.: Image Analysis and Mathematical Morphology, vol. 2. Academic Press, London (1988)
34. Soille, P.: Morphological Image Analysis, 2nd edn. Springer, Berlin (2003)
35. van den Boomgaard, R.: Mathematical Morphology: Extensions Towards Computer Vision. PhD thesis, University of Amsterdam, The Netherlands (1992)
36. Weickert, J.: Coherence-enhancing diffusion of colour images. In: Sanfeliu, A., Villanueva, J.J., Vitrià, J. (eds.) Proc. Seventh National Symposium on Pattern Recognition and Image Analysis, Barcelona, Spain, April 1997, vol. 1, pp. 239–244 (1997)
37. Weickert, J.: Coherence-enhancing diffusion filtering. International Journal of Computer Vision 31(2/3), 111–127 (1999)
38. Weickert, J., Brox, T.: Diffusion and regularization of vector- and matrix-valued images. In: Nashed, M.Z., Scherzer, O. (eds.) Inverse Problems, Image Analysis, and Medical Imaging. Contemporary Mathematics, vol. 313, pp. 251–268. AMS, Providence (2002)
39. Weickert, J., Hagen, H. (eds.): Visualization and Processing of Tensor Fields. Springer, Berlin (2006)